1-1-1977

Stress rupture behavior of a unidirectionally solidified Ni/Ni 3Al-Ni3Nb eutectic composite.

Xuan Nguyen-Dinh

STRESS RUPTURE BEHAVIOR OF A UNIDIRECTIONALLY SOLIDIFIED Ni/Ni_3Al-Ni_3Nb EUTECTIC COMPOSITE

by

Xuan Nguyen-Dinh

A Thesis

Presented to the Graduate Faculty

of Lehigh University

in Candidacy for the Degree of

Master of Science

in

Metallurgy and Materials Science

Lehigh University

1977

This thesis is accepted and approved in partial fulfillment of the requirements for the degree of Master of Science.

December 17, 1976
(date)

Professor in Charge

Co-Director

Chairman of Department

ACKNOWLEDGEMENT

The author wishes to acknowledge the guidance and encouragement of Professor R. W. Hertzberg and Professor R. W. Kraft. He is indebted to his wife Stephanie for her patient collaboration during the typing of the manuscript.

The assistance of Messrs. D. Bush, M. Sheska and the machine shop personnel was also appreciated. The author wishes to acknowledge Bethlehem Steel Corporation who performed the machining of the specimens employed during the current investigation. Mr. R. Whitney, in behalf of Carpenter Technology Corporation, donated four bars of extruded IN-100 from which the extension rods of the creep testing system were machined.

Finally, the author also gratefully acknowledges the initial financial support of Brown-Boveri Research Center, Baden (Switzerland) and additional financial support of the National Aeronautics and Space Administration under Grant NGR-39-007-007.

TABLE OF CONTENTS

TABLE OF CONTENTS (cont'd.)

LIST OF FIGURES

LIST OF FIGURES (cont'd.)

LIST OF FIGURES (cont'd.)

LIST OF FIGURES (cont'd.)

ABSTRACT

The stress rupture behavior of a Ni/Ni_3Al-Ni_3Nb (Ni-21.5 wt. % Nb-2.5 wt. % Al) directionally solidified eutectic composite grown at 5 cm/hr was investigated in the temperature range 480 to 950°C.

The microstructure of the aligned eutectic composite consisted of Ni (γ) lamellae strengthened by Ni_3Al (γ') precipitates and reinforced by Ni_3Nb (δ) lamellae.

An attempt was made to relate the deformation and fracture mechanisms which occurred during stress rupture testing to the three deformation and fracture mechanisms identified by Bertorello, et al in their investigation of the hot tensile properties.

Under short time 550°C stress rupture (less than 100 hours), the eutectic composite deforms by slip in the γ phase, by twinning in the δ phase on $\{211\}$ type planes and by cracking at the δ twin - δ matrix interface. Failure was caused by the link up of these cracks and by eutectic grain boundary delamination limited to a region near the fracture surface. Grain boundary delamination was observed to be the result of premature rupture of the brittle γ' film at the eutectic grain boundaries which caused transverse cracks to be deflected. This Region I deformation and fracture behavior in stress rupture is similar to Region I tensile deformation and fracture behavior which was found to

operate in the temperature range 20 to 400°C.

At intermediate exposure time at 550°C, additional grain boundary delamination occurred away from the fracture surface. Deformation and fracture behavior in this Region II was also observed under tensile conditions from 400°C to 690°C.

Under long time exposure at 550°C cooperative twinning of the γ and δ phases occurred, resulting in the appearance of two variants of deformation bands. Bertorello, et al have also observed the same deformation behavior during tensile testing between 690°C and 926°C.

Minimum creep rates were measured in the temperature range 480 to 580°C and yielded a value of 380 kjoules/mole for the activation energy of the creep process. The significance of this result was discussed in terms of known activation energy data. It was proposed that the grain boundary delamination process might be rate-controlling during steady-state creep, and therefore would contribute to the creep of the eutectic composite.

Unlike the γ-δ system, at 750°C the stress rupture behavior of γ/γ'-δ eutectic composite was characterized by a transition from Region I behavior to a void nucleation and void coalescence process.

The 850°C stress rupture behavior and the long time 950°C stress rupture behavior were characterized by void nucleation and void coalescence, with the

highest creep ductility being related to the highest amount of voids produced during composite deformation.

A longitudinal section of a short time 950°C stress rupture specimen exhibited features characteristic of Region II tensile behavior.

CHAPTER I

INTRODUCTION

1.1 Introduction to High Temperature Materials.

The development of Ni and Co-base superalloys has played an important role in the increased performance of the aircraft gas turbine (1). These materials derive their high temperature capability by several strengthening mechanisms: solid solution hardening by addition of Ta, Nb, Mo, W, Cr for example; dispersion strengthening by carbides of these elements; and age hardening by precipitation of ordered intermetallic phases such as γ', γ'', η or δ .

Conventional superalloy turbine blades have equiaxed grain structure. At high temperatures, the grain boundaries that are normal to the major stress axis are preferential sites for crack nucleation and propagation which results in the failure of the part. Directional solidification of superalloys provided a means to eliminate these grain boundaries. Indeed, nickel based alloys containing columnar grains and monocrystals were successfully produced by this novel process and were found to have longer creep rupture life, higher creep ductility and better thermal shock resistance than their conventional counterparts (2-5).

One crucial problem of conventional and directionally solidified superalloys is the resolutioning of the

strengthening phases upon exposure at high temperatures. From the standpoint of the engine designer, engine performance can be increased by increasing turbine inlet temperature. The phase stability problem concomitant to a good retention of strength and ductility seems to be solved in directionally solidified eutectics.

In the early sixties, Kraft and his co-workers (6-10) discovered that in-situ composites can be produced by unidirectionally solidifying binary eutectics. Coupled plane front growth, established under specific conditions of growth rate, temperature gradient at the solid-liquid interface and purity of the elements, resulted in an aligned lamellar or fibrous biphase anisotropic structure which exhibited a composite behavior. Unlike in man-made composites, microstructures of directionally solidified binary eutectics exhibited thermal stability when exposed to temperatures close to their melting points, due to the presence of low energy interfaces established under growth conditions approaching equilibrium (11-17).

Subsequently, coupled plane front growth was successfully achieved for other binary and pseudo-binary eutectics, for off-eutectic compositions which allowed variation of the volume fraction of the phases, and for monovariant eutectics which permitted variation of the volume fraction and composition of the phases (18-28).

Nevertheless, multivariant, multicomponent

eutectic systems (29-41) appeared to be the short term answer to the requirements of the turbine designer since the increased flexibility in varying the volume fraction and the chemistry of the phases provided a means to produce materials whose matrices can be strengthened by mechanisms similar to those found in conventional superalloys.

1.2 Objectives of the Current Investigation.

In an extensive study, Gangloff and Hertzberg (24) identified three deformation and fracture mechanisms which govern the hot tensile and creep behavior of the unidirectionally solidified Ni-Ni_3Nb eutectic composite.

In tensile testing between 25°C and 600°C and in short time 600°C stress rupture testing, the eutectic composite deforms by twinning of the δ,(Ni_3Nb) phase on $\{211\}$ type planes and by twin boundary cracking. Fracture occurs by the coalescence of sub-critical δ phase cracks.

Cooperative twinning of the δ and γ phases was found to operate in tension between 600°C and 875°C, during long time creep exposure at 600°C and short time creep testing at 750°C. Coalescense of sub-critical cracks along transgranular bands of γ and δ twins promoted fracture of the eutectic composite.

Under 875°C and 1000°C tensile conditions and upon long time creep exposure at 750°C, deformation was caused by void nucleation at lamellae ends and eutectic

grain boundaries while fracture was due to void coalescence into transgranular cracks.

It was concluded that, in the unidirectionally solidified Ni-Ni_3Nb eutectic composite, there existed a time-dependent transition of the deformation and fracture processes in creep which was analogous to a temperature-dependent transition in tensile deformation and fracture, the transition in creep occurring at a shorter time as the testing temperature was increased.

In a recent study of the hot tensile properties of a γ/γ'-δ (Ni-21.5 wt% Nb-2.5 wt% Al) eutectic composite grown at 5 cm/hr., Bertorello et al (40) identified three regions of deformation and fracture behavior. In Region I, from 20°C to 400°C, deformation of the eutectic composite was caused by twinning and cracking of the δ phase, and by slip in the γ phase. This deformation behavior was similar to that observed at low temperatures in the γ-δ eutectic composite.

Furthermore, it was found that extensive grain boundary delamination occurred in a region near the fracture surface. The investigators proposed that premature rupture of the brittle γ' film at the eutectic grain boundaries caused the transverse cracks to be deflected. Grain boundary delamination was found at the fracture surface and along the gage length of specimens tested in the temperature range from 400°C to 690°C.

In this Region II tensile deformation mode, it was found that the considerable ductility of 27% observed at 550°C could be related to the previously recognized ductility minimum of γ' and its key role in the delamination process. It was suggested that the critical temperature range 600-750°C associated with the ductility minimum of γ' strengthened superalloys could be depressed by addition of niobium.

Region III tensile deformation behavior, found to operate from 690°C to 926°C was related to the cooperative twinning of the γ and δ phases.

The purposes of the current investigation are threefold:

i) to establish the stress rupture response of the eutectic composite studied by Bertorello et al,

ii) to identify those mechanisms which promote deformation and fracture of the eutectic allov during stress rupture testing, and possibly to relate these mechanisms to those defined by the hot tensile properties investigation, and

iii) to measure the activation energy for the creep process in the temperarure range where Region II behavior is operative.

CHAPTER II

EXPERIMENTAL PROCEDURE

2.1 Melting and Solidification

Solidification procedures employed during this study were similar to techniques described by Gangloff (23) and Mills (26). Niobium of 99.8% purity, purchased in 1 cm. diameter bar was cut into cylinders which were subsequently ultrasonically degreased in methanol. Aluminium of 99.99% purity was cut into 1 cm. cubes, then cleaned by methanol. Nickel, purchased as 3 cm. X 4 cm. X 1.5 cm. slabs was pickled in a solution of 1 part H_2O, 1.5 parts H_2SO_4, 2.5 parts HNO_3, 10 to 30 grams of NaCl and 0.25 part of HF.

Several 2 kg. master heats of composition 21.5 wt % Nb - 2.5 wt % Al - balance Ni were induction melted in an alumina crucible placed in an Inducto vacuum induction melting furnace powered by a 30 kW motor generator. The system was pumped down to 2.66 Pa, then backfilled with argon to provide an inert atmosphere at positive pressure. The niobium was placed at the bottom of the crucible. Power to the crucible coil was gradually increased until melting of the nickel and niobium was achieved. Aluminium was then poured into the melt. After five to ten minutes of homogenization, the power to the crucible coil was switched off. Then

the molten charge was poured into a steel split mold to produce eight round bars 1.25 cm. in diameter by 15 cm. long. Prior to casting, the mold walls were coated with a wash consisting of MgO powder in ethyl alcohol, and placed in a furnace at 200°C.

The as-cast bars were cleaned in the previously described pickling solution, then unidirectionally solidified in 95.5% pure aluminium oxide crucibles under a vacuum purged, positive argon pressure at a growth rate of 5 cm./hr. Solidification was achieved in a vertical zone melter equipped with an induction coil and a water cooled chuck which provided a high thermal gradient (26).

2.2 Stress Rupture Testing

Stress rupture specimens (9.318 cm. diameter, 1.78 cm. gage length) shown in Figure 1 were machined from the unidirectionally solidified bars. When the longitudinal structure was deemed satisfactory upon metallographic examination, the bar was machined to yield two test specimens.

Constant load testing according to ASTM specification E 139-69 was conducted in air on Satec stands and on Dennision stands equipped with Marshall test furnaces. Temperature was controlled to within $\pm$ 5°C by means of two chromel-alumel thermocouples wired to the specimen. Elongation was measured on the fractured halves of the specimen. Testing on the

Satec stands allowed continuous recording of elongation by a system consisting of an extensometer clamped on the shoulders of the specimen, a linear voltage differential transformer (LVDT), a demodulator and a multi-point chart recorder. Because testing was performed in air and oxidation may result in excessive scaling of the extensometer, the previously described system was used for temperatures under 750°C. In several instances, because of the instability of the output signal, elongation was measured on the fractured halves.

2.3 Metallography

Fracture surfaces were plated in a nickel plating bath (5 parts Enplate NI-415 A, 1 part Enplate NI-415 B, 8 parts water) at 85°C, then cut longitudinally by electrodischarge machining. Longitudinal sections were mounted in bakelite, polished through 600-grit wet polishing papers, 6 micron-1 micron diamond pastes, 0.3-0.6 micron alumina powders and electropolished in a solution consisting of 37 parts H_3PO_4, 56 parts glycerin and 7 parts water, with a voltage of 10 volts accross the electrodes.

CHAPTER III

PRESENTATION AND DISCUSSION OF RESULTS

3.1 Microstructure and Crystallography

The composition of the alloy chosen for the present study was 21.5 wt % Nb, 2.5 wt % Al and balance Ni. Upon solidification, the liquid separates into two solid phases, the face-centered cubic γ-Ni solid solution and the orthorhombic δ-Ni_3Nb phase. Figure 2 shows a representative transverse section of the microstructure. Also shown is the presence of γ'-Ni_3Al precipitates obtained by precipitation from the Ni solid solution upon cooling from the solidus temperature. Lemkey and Thompson (37, 38) have determined that the crystallographic habit of the γ/γ'-δ alloys is:

$$\text{growth} \parallel [011]_\gamma \parallel [100]_\delta$$
$$\text{interface} \parallel (1\bar{1}1)_\gamma \parallel (010)_\delta$$

3.2 Stress Rupture Behavior

The testing program is summarized in Table 1. Figure 3 is a stress-time to rupture plot which shows the effect of temperature and initial stress level on the stress rupture life and depicts the expected increase in stress rupture life with decreasing applied stress. A Larson-Miller parameter plot shown in figure 4 compares the results of the present study with those obtained by United Aircraft Research Laboratories for a γ/γ'-δ alloy (Ni-21.75 wt % Nb-2.55 wt % Al) grown at 38 cm./hr. (The empirical constant in the Larson-Miller

Parameter in both cases was assumed to be 20). At this stage of our understanding of eutectic composite behavior, it is not certain that the Larson-Miller Parameter is the best comparison criterion; similarly, the material constant in the relation Parameter = T (C + log t) taken as 20, may not represent the best fit for this alloy. As seen in figure 4, the UARL alloy is superior to the alloy prepared for this investigation. It is not surprising to find such a difference since Thompson et al (25) demonstrated that reduction of the lamellar spacing increased the creep resistance of the eutectic composite. In fact, if the Larson-Miller plot is normalized relative to tensile strength, the two sets of data are in better agreement (figure 5).

It was shown that the minimum creep rate (steady state creep rate) of lamellar eutectic composites (25, 38) follows the relation:

$$\dot{\varepsilon}_{ss} = k\ (\sigma^n/T)\ \exp\ (-\frac{\Delta H}{RT})$$

where k = material constant

n = creep exponent

T = absolute temperature (^oK)

ΔH = activation energy (joules/mole)

R = universal gas constant = 8.314 joules/mole-deg.

Table 2 gives the minimum creep rate of three specimens tested at the same stress level and at different temperature. Based on the previously described

relationship between minimum creep rate and temperature, the temperature compensated creep rate was computed from the data of Table 2 and plotted on a log-log scale with respect to (1/RT), see figure 6. Using a least mean squares method, a straight line was drawn through the data points. The slope of the line yields the activation energy for the creep process and is equal to 380 kjoules/mole.

A value of 349 kjoules/mole for the creep activation energy of $\gamma/\gamma'-\delta$ alloys was reported by Breinan (41). Although the value found during this investigation is in agreement with Breinan's result, it is not possible to ascertain conclusively as to which phase is in fact controlling the creep process in the temperature range 480 to 580°C owing to the paucity of creep activation energy data. For example, the generally accepted activation energy for steady-state creep of pure Ni is 276 kjoules/mole while the values associated with the creep of the intermetallic compounds Ni_3Nb and Ni_3Al are respectively 657 kjoules/mole and 685 kjoules/mole (47). Furthermore, Ni_3 (Al, Mo) was found to have an activation energy of 446 kjoules/mole (48) whereas creep activation energy data for Ni_3Al containing Nb or Ni_3Nb containing Al have not been reported yet.

In the hot tensile properties investigation by Bertorello, et al (40), it was found that the γ' film at the eutectic grain boundaries played an important role

during tensile deformation at 550°C. It was shown that rupture associated with the γ' film allowed the deflection of transverse cracks to occur along the direction of the major stress axis, resulting in an increase in ductility. The hypothesis that this grain boundary delamination process is rate-controlling during steady-state creep cannot be ruled out; therefore it would be expected that the γ' grain boundary film would contribute to the creep of the eutectic alloy in the 550°C temperature range.

3.3 Deformation and Fracture Mechanisms

3.3.1 Deformation and Fracture in the Low Temperature Range (480°C to 580°C)

It was reported elsewhere (22, 23, 24) that in the γ-δ eutectic composite the intermetallic Ni_3Nb deforms by twinning on $\{211\}$ type planes while the Ni phase slips during deformation of the composite. Figures 7 and 8 give evidence that the same deformation mechanism occurs during exposure up to 700 hours in the temperature range 480°C to 580°C. Note the slip markings in the γ lamellae and the way the cracks propagate at the δ twin- δ matrix interface. Failure of the eutectic occurred by the link up of these cracks and by eutectic grain boundary delamination, as depicted in figures 9 and 10.

Specimen L6-5 which failed after less than 100 hours exposure at 550°C shows grain boundary

delamination at the fracture surface (figure I0 a) characteristic of Region I tensile deformation (40).

At intermediate exposure time at 550°C, grain boundary delamination occurs also away from the fracture surface (figure 10 b), the extent of which is less than that found on specimens deformed in Region II tensile behavior (40). Bertorello et al proposed that the ductility maximum of 27% obtained during tensile deformation at 550°C could be attributed to premature fractures associated with the γ' grain boundary film at 550°C which permitted the structure to deflect transverse cracks by grain boundary delamination. The ductility found on specimen J2-5-2 (about 7%) can be rationalized on the basis of this proposed deformation mechanism.

Figure 11 shows that δ phase twin density is approximately equal in both Region I and Region II creep specimens, whereas cracking is more evident in Region II creep specimens.

Under long time exposure at 550°C, a transition from Region II deformation behavior to Region III deformation behavior occurred. Longitudinal sections showed two variants of deformation bands (figure 12), consisting of colinear γ and δ twins (23, 24, 40). Note that the δ twin density has decreased markedly. This cooperative twinning process is quite similar to that found in the γ-δ eutectic composite after long

time 600°C and short time 750°C creep (23, 24). Metallographic observation revealed that cooperative twinning occurred in the γ/γ'-δ eutectic composite to a lesser extent than in the γ-δ eutectic alloy. It is believed that, because of the γ' precipitates, the γ phase cannot deform readily by twinning in conjunction with the twinning of the δ phase.

3.3.2. Deformation and Fracture at 750°C

Under 750°C stress rupture conditions, longitudinal sections of specimens which exhibited a rupture life of less than 100 hours showed that composite deformation occurred by twinning in the δ phase and by grain boundary delamination limited to a region near the fracture surface (figure 13). The δ phase twins appeared to be thinner, resulting in a drastic decrease in the frequency of cracking at the δ twin-δ matrix interface. Deformation under short time 750°C stress rupture conditions is thus typical of Region I tensile deformation.

The deformation mechanism observed from metallographic examination of long time 750°C stress rupture specimens was characterized by void nucleation at lamellae ends and eutectic grain boundaries. Figure 14 a shows that fracture occurred by the link up of these voids. It is believed that, because of the disruption of the crystallographic relationships at lamellae ends and eutectic grain boundaries, these

sites have a high energy configuration and would become preferred sites for void nucleation during composite deformation.

Metallographic analysis of two specimens creep tested at 760°C which failed after less than 100 hours of exposure revealed that cooperative twinning of the δ and γ phases became operative. Near the fracture surface, severe blocky movements of the γ and δ lamellae produced cracking in the two phases (figures 15 b and 16). This extremely localized deformation mechanism resulted in failure of the composite when these cracks linked up, thereby decreasing the load bearing capability of the specimen. It was noted that away from the fracture surface, deformation of the composite was less severe, with fine bands of colinear γ and δ twins being observed (figure 15 a). It is believed that this γ-δ cooperative twinning deformation mechanism was not induced by a change in the testing temperature from 750°C to 760°C, but rather by some unidentified metallurgical variable.

3.3.3 Deformation and Fracture at 850°C and 950°C

Composite deformation under 850°C and 950°C bear some resemblance to the previously described long time 750°C deformation mechanism (figures 17 a and 19 a), with the difference that creep ductility was higher for all test conditions at 850°C and for long time 950°C creep specimens. The increase in creep ductility was

related to an increase in the number of voids as clearly evidenced in figure 19 a.

Metallographic analysis of a short time 950°C creep specimen (specimen M5-5-1) showed that composite deformation was qualitatively similar to Region II tensile behavior: the δ phase deformed by twinning and cracking (figure 18 b), whereas grain boundary delamination was believed to be the result of the coalescence of small voids produced at eutectic grain boundaries. This type of delamination appears to be different from that found in Region I hot tensile deformation behavior, 550°C and short time 750°C creep exposure.

Two additional observations were considered important to mention. Longitudinal section of specimen K4-5 crept under 850°C exhibited δ Widmanstatten precipitates in the γ/γ' phase (figure 17 b). δ Widmanstatten precipation was previously reported (50) for the $\gamma-\delta$ aligned eutectic as a result of a 1220°C solution treatment and long time static exposure at 800°C.

Metallographic observation gave evidence that long time exposure under high temperature produced coarsening of the γ' precipitates (figure 19 b). This observation suggests that, in order for $\gamma/\gamma'-\delta$ eutectic alloys to retain their high strength at elevated temperatures, further alloying with elements which would stabilize the Ni_3Al precipitates will be required.

CHAPTER IV

CONCLUSIONS

Several conclusions were drawn from this study :

i) At 550°C, the stress rupture behavior of the eutectic alloy was characterized by three deformation and fracture mechanisms which were qualitatively similar to the three deformation and fracture mechanisms identified by Bertorello, et al in their investigation of the hot tensile properties. The time-dependent transition in creep and the temperature-dependent transition in tensile deformation suggest that the 550°C stress rupture behavior of the $\gamma/\gamma'-\delta$ eutectic composite bears some similarity with the elevated temperature tensile and creep rupture behavior of the $\gamma-\delta$ eutectic composite.

ii) The creep activation energy of the eutectic composite tested between 480°C and 580°C was found to be 380 kjoules/mole.

iii) Unlike the $\gamma-\delta$ system, at 750°C the stress rupture behavior of the $\gamma/\gamma'-\delta$ eutectic composite was characterized by a transition from Region I behavior to a void nucleation and void coalescence process. At 760°C, it was found that

cooperative twinning of the γ phase and δ phase became operative. It was hypothesized that this cooperative twinning process was caused by some unidentified metallurgical variable rather than by a change in the testing temperature.

iv) The 850°C stress rupture behavior and the long time 950°C stress rupture behavior were characterized by void nucleation and void coalescence, with the highest creep ductility being related to the highest amount of voids produced during composite deformation.

A longitudinal section of a short time 950°C stress rupture specimen exhibited features characteristic of Region II tensile behavior.

v) The current study showed that the deformation and fracture mechanisms reported by Gangloff and Bertorello et al have been identified in this study. The analogy between a temperature-dependent transition in tensile deformation and fracture, and a time-dependent transition of the deformation and fracture processes in creep which was found for the γ-δ aligned eutectic was not always found for the γ/γ'-δ directionally solidified eutectic at high

temperatures.

TABLE 1

CREEP RUPTURE DATA

Specimen*	Temperature °C	Stress MPa	(ksi)	Time To Rupture hrs	Elongation (%)
M4-5-1	480	967	(138.5)	718.1	2.6**
I5-5-1	495	911	(130.4)	55.5	5.1**
M1-5-1	530	982	(140.6)	52.9	4.5**
L6-5	547	942	(134.9)	87.7	2.4**
I6-5-1	550	840	(120.2)	1055.7	0.7
J2-5-2	553	978	(140.0)	397.9	6.9
M6-5-1	578	967	(138.5)	53.1	4.6**
L4-5-1	550	911	(130.4)	(574)***	-
K2-5	653	868	(124.3)	183.6	1.7**
I5-5-2	750	699	(100.0)	13.7	1.3
I4-5-1	754	699	(100.0)	52.4	1.2
J1-5-2	750	629	(90.0)	22.2	0.9
M2-5	750	586	(83.9)	390.8	0.9**
J3-5-2	748	562	(80.4)	200.7	-
K3-5-1	750	543	(77.8)	247.7	0.9**
J1-5-1	750	524	(75.0)	261.0	1.2
I4-5-2	760	765	(109.5)	12.3	2.4
J2-5-1	760	638	(91.3)	54.2	0.1
K4-5	850	350	(50.1)	105.1	7.0
J7-5	850	455	(65.2)	29.3	6.0
J3-5-1	930	242	(34.6)	32.9	0.7
M5-5-1	950	177	(25.3)	12.0	2.0
L5-5-2	950	154	(22.0)	120.2	-
I7-5-2	950	132	(18.9)	272.6	13.6

* Third number identified the position of the specimen with respect to the ingot: "1" for the tail, "2" for the head.

** Elongation measured by extensometer.

*** Test stopped at time reported.

TABLE 2

MINIMUM CREEP RATE DATA

Specimen	Stress MPa	(Ksi)	Temperature °C	Minimum Creep Rate ($\times 10^{6}$ hr $^{-1}$)
M4-5-1	967	(138.5)	480	0.498
M1-5-1	982	(140.6)	530	54.765
M6-5-1	967	(138.5)	578	458.00

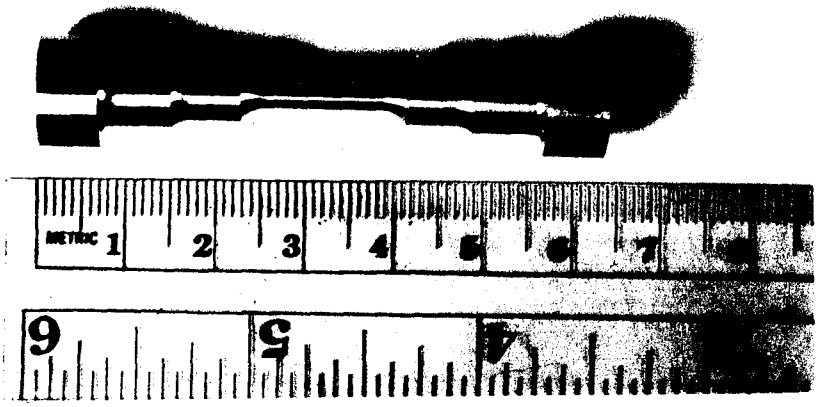

Figure 1: Creep Rupture Specimen

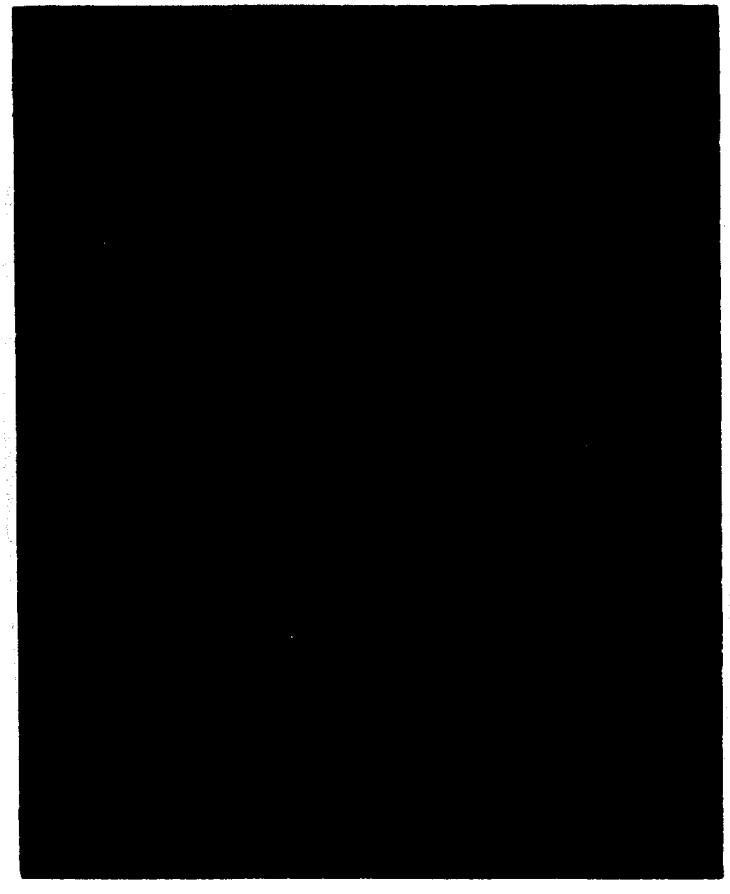

Figure 2: Representative microstructure of a transverse section of a γ/γ'-δ eutectic composite grown at 5 cm/hr. Electropolished. Magnification 1600X.

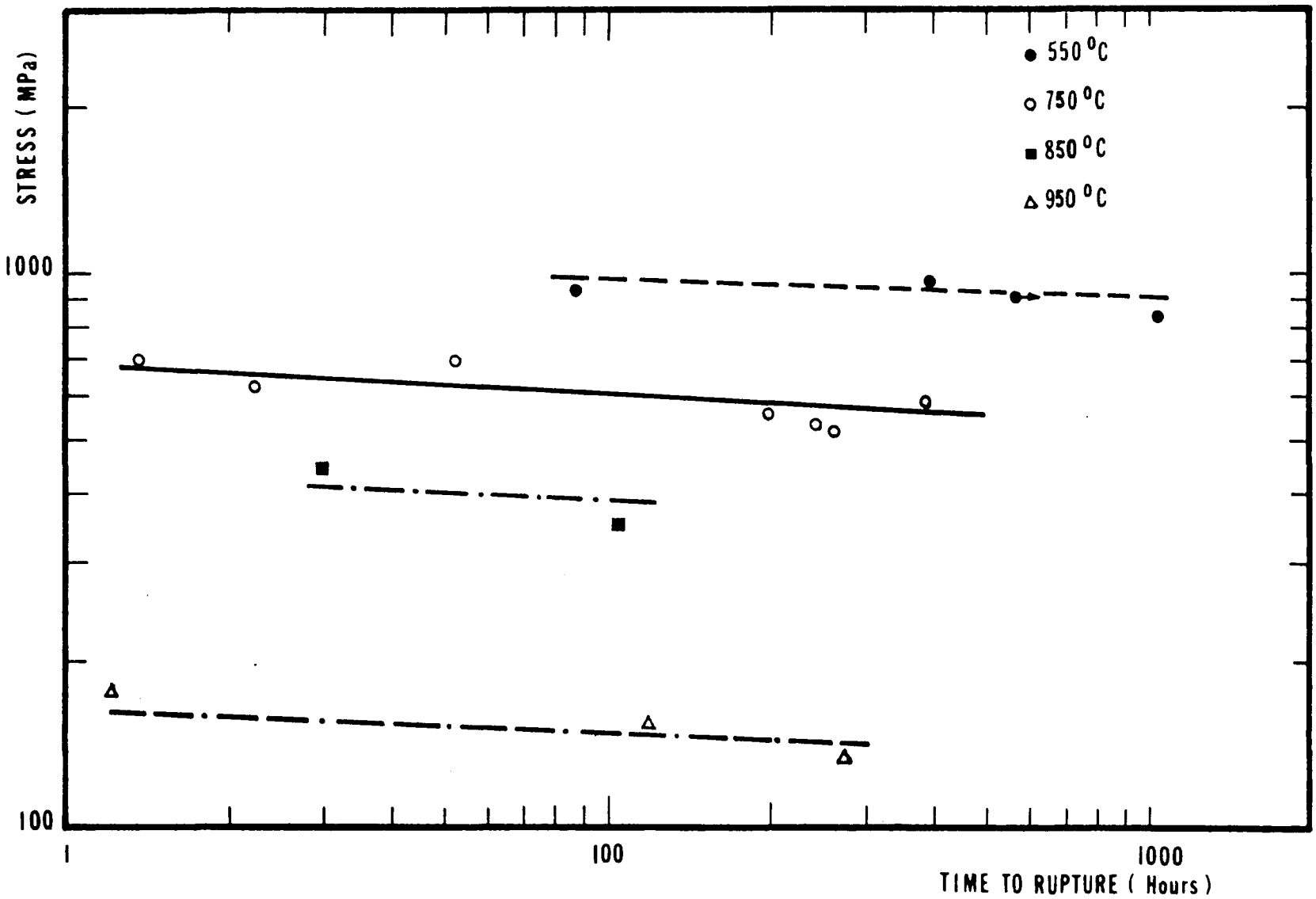

Figure 3: Stress-rupture time data of Ni-21.5 wt. % Nb-2.5 wt. % Al eutectic composite.

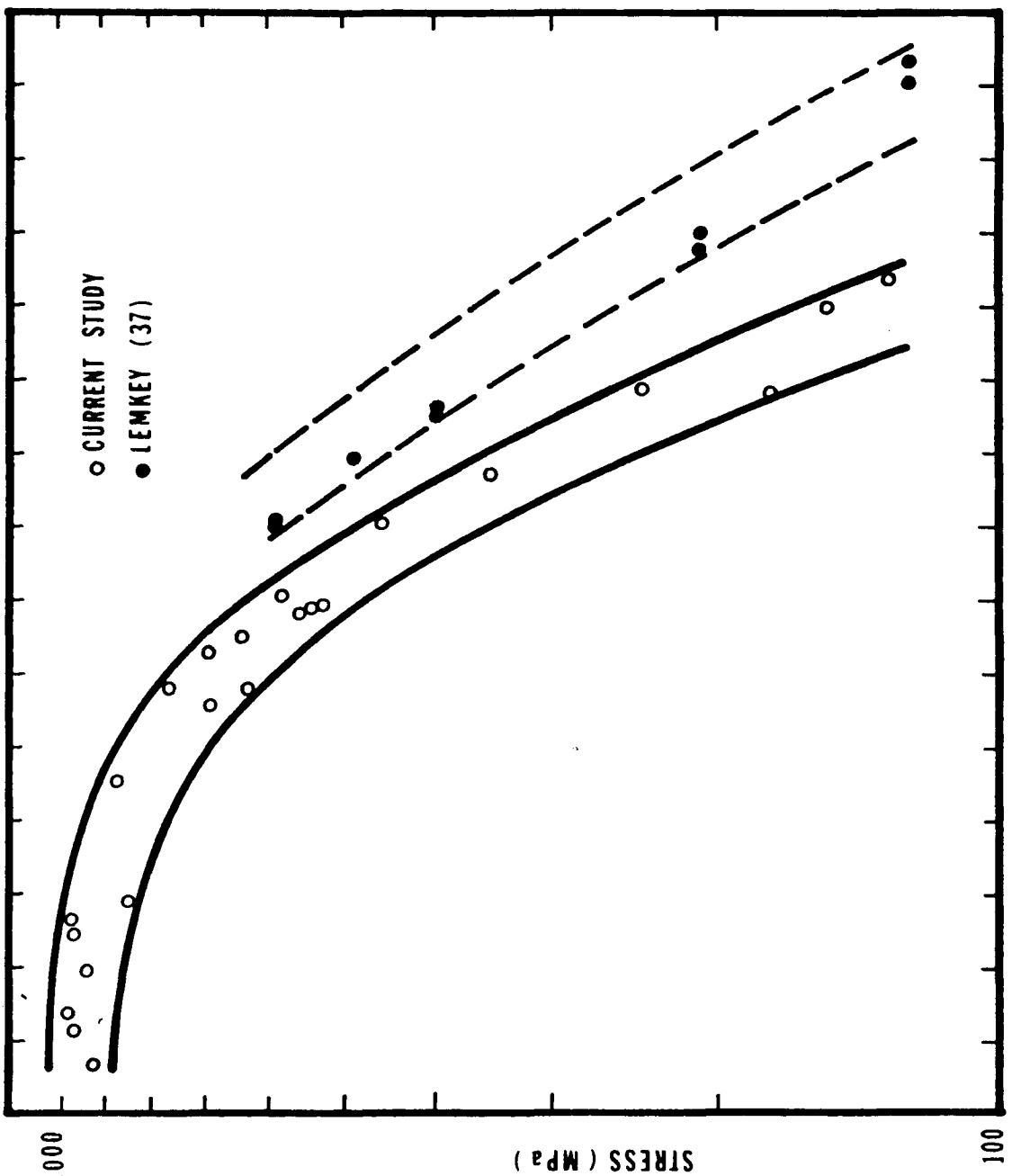

Figure 4: Larson-Miller parameter plot of Ni-Nb-2.5 wt. % Al alloys.

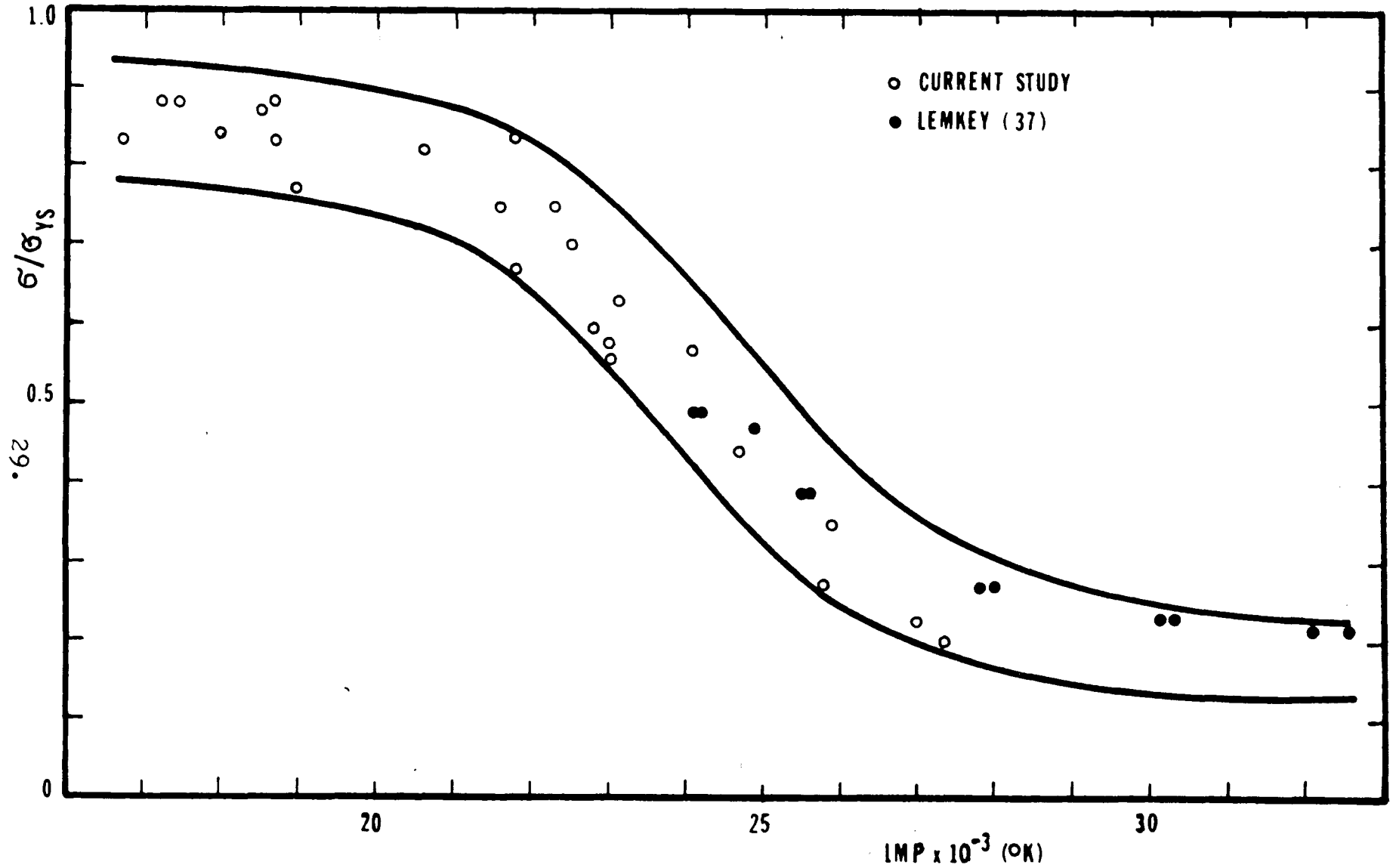

Figure 5: Normalized Larson-Miller parameter plot of Ni-Nb-2.5 wt. % Al alloys.

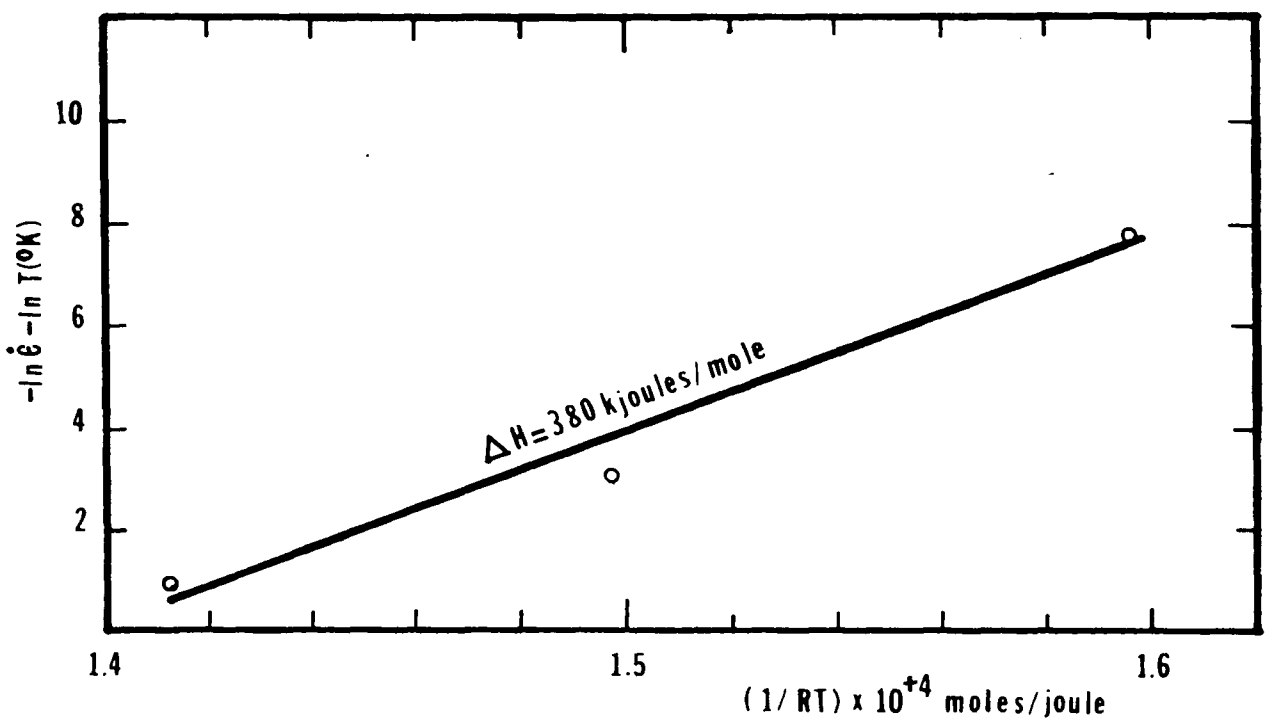

Figure 6: Temperature compensated minimum creep rates as a function of (1/RT).

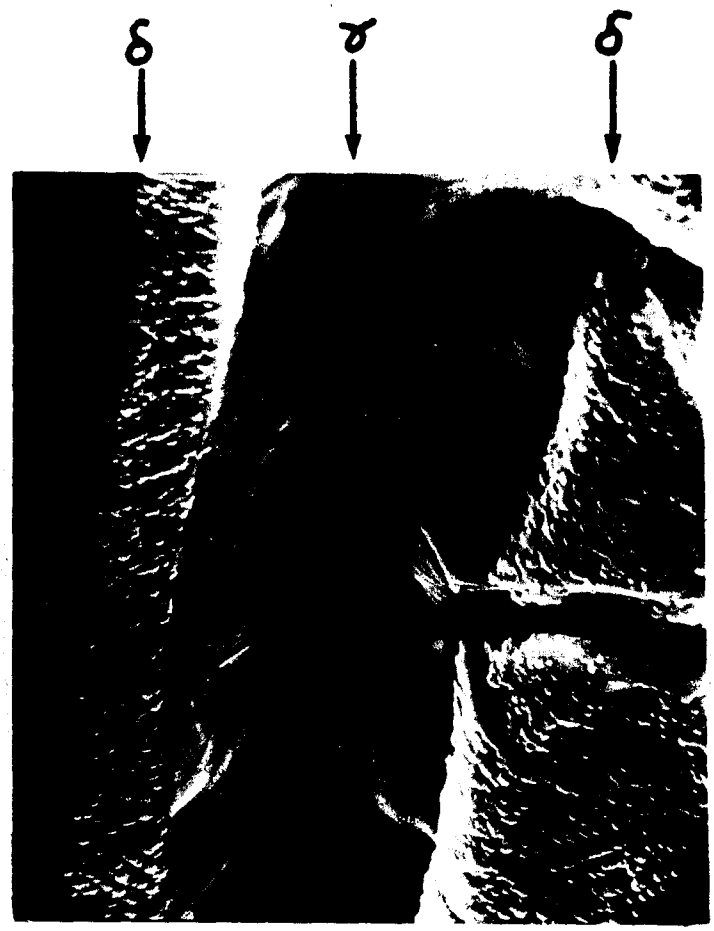

Figure 7: Scanning Electron Micrograph of a 530°C stress rupture fracture (Specimen M1-5-1) revealing slip markings in a γ phase lamella and cracking in a δ phase lamella . Magnification 6080X.

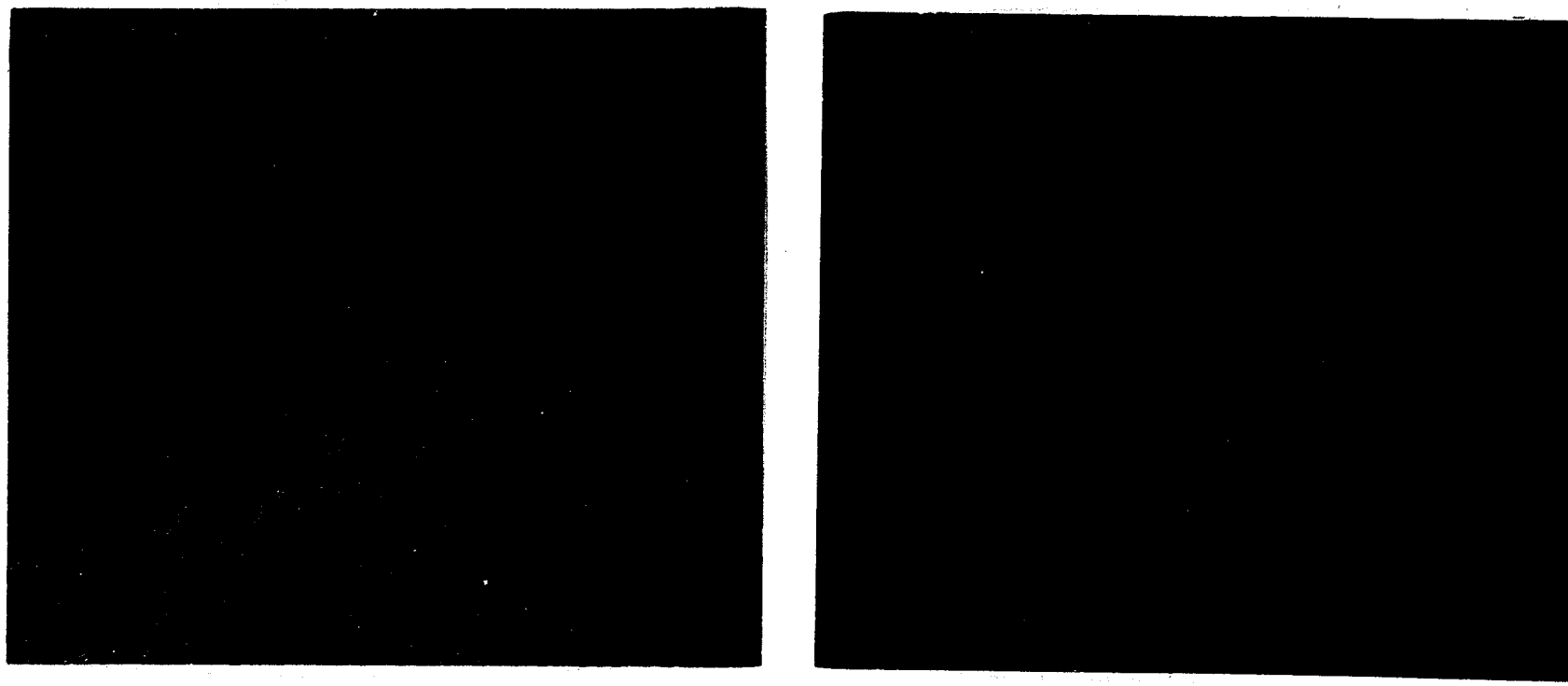

(a) (b)

Figure 8: Longitudinal sections depicting δ phase twins. Electropolished.

(a) Specimen M4-5-1. Note the way the cracks propagate in the δ phase. Magnification 400X.

(b) Specimen J2-5-2. Note the even distribution of δ phase twins and the fine distribution of the γ' precipitates. Magnification 1000X.

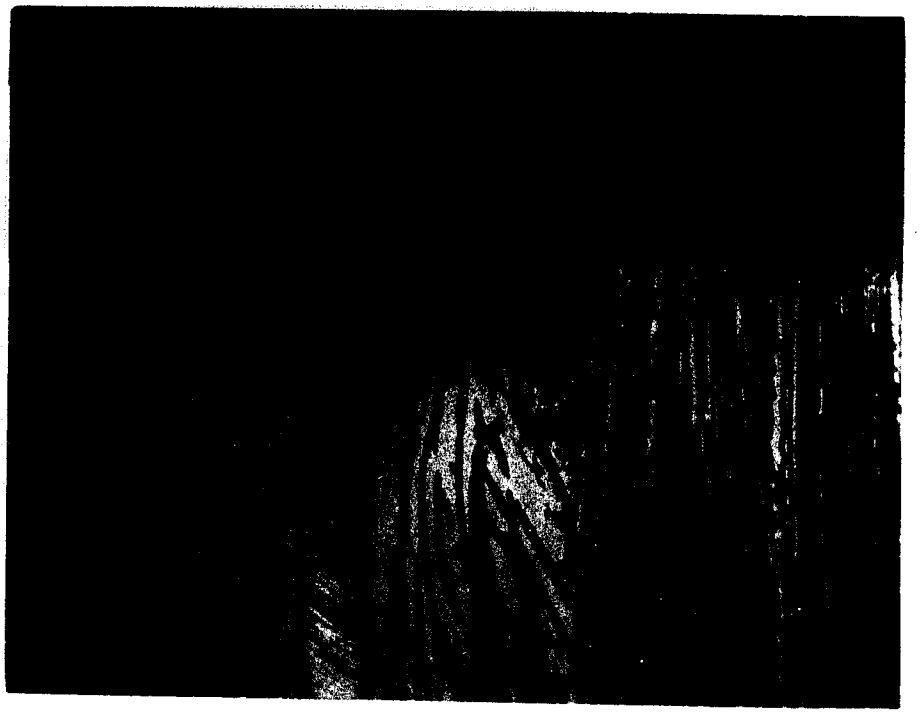

Figure 9: Longitudinal fracture profile of a 495°C stress rupture fracture (Specimen I5-5-1). Electropolished. Magnification 100X.

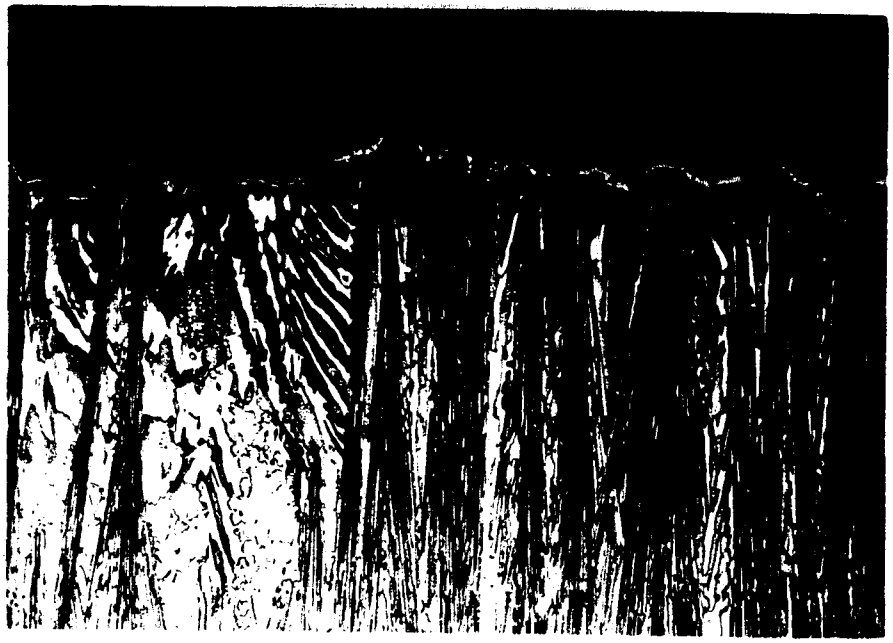

(a)

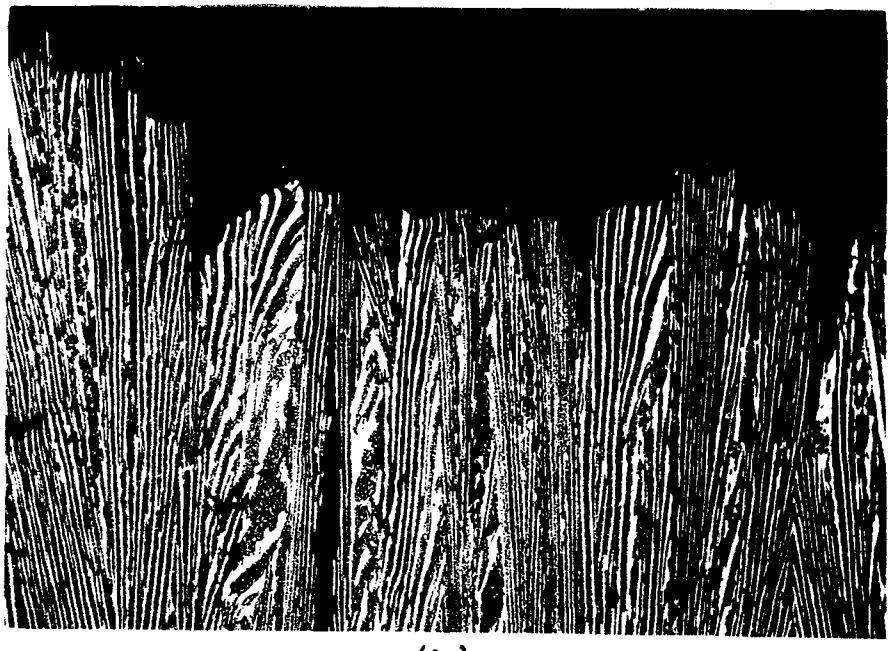

(b)

Figure 10: Longitudinal fracture profiles of two 550°C stress rupture specimens. Electropolished.

(a) Specimen L6-5. Magnification 100X.
(b) Specimen J2-5-2. Note the higher amount of delamination. Magnification 100X.

(a) (b)

Figure 11: Longitudinal sections of two 550°C stress rupture specimens revealing δ phase twinning. Electropolished.

(a) Specimen L6-5. δ phase cracking is not evident. Magnification 320X.

(b) Specimen J2-5-2. Note extensive cracking at δ phase twin-δ phase matrix interface. Note eutectic grain boundary delamination produced by transverse cracks. Magnification 320X.

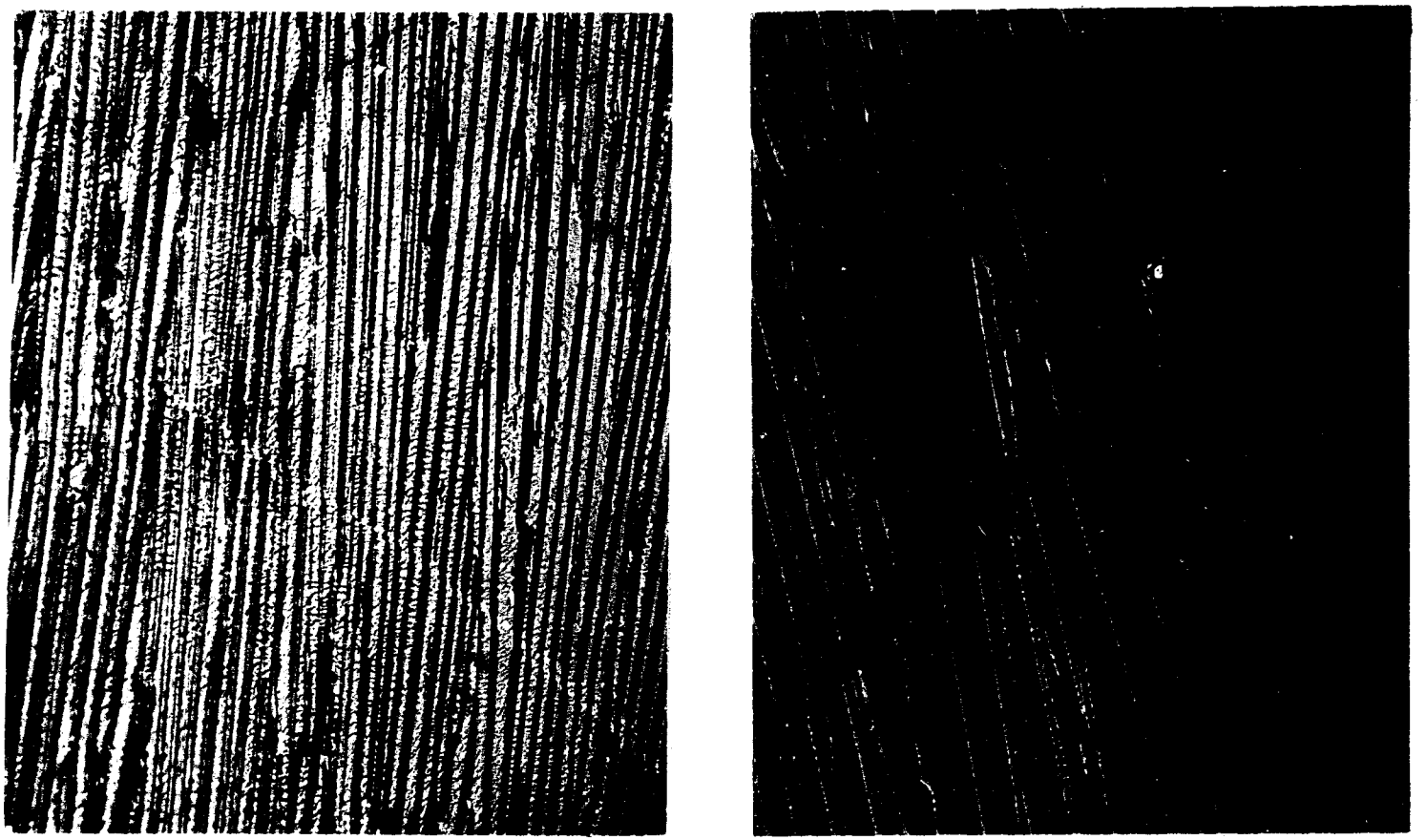

(a) (b)

Figure 12: Longitudinal section of a long time 550°C stress rupture specimen (Specimen I6-5-1) showing the cooperative twinning of the γ and δ lamellae. Electropolished.

(a) Note the two varients of deformation bands. Magnification 625X.

(b) Magnification 1000X.

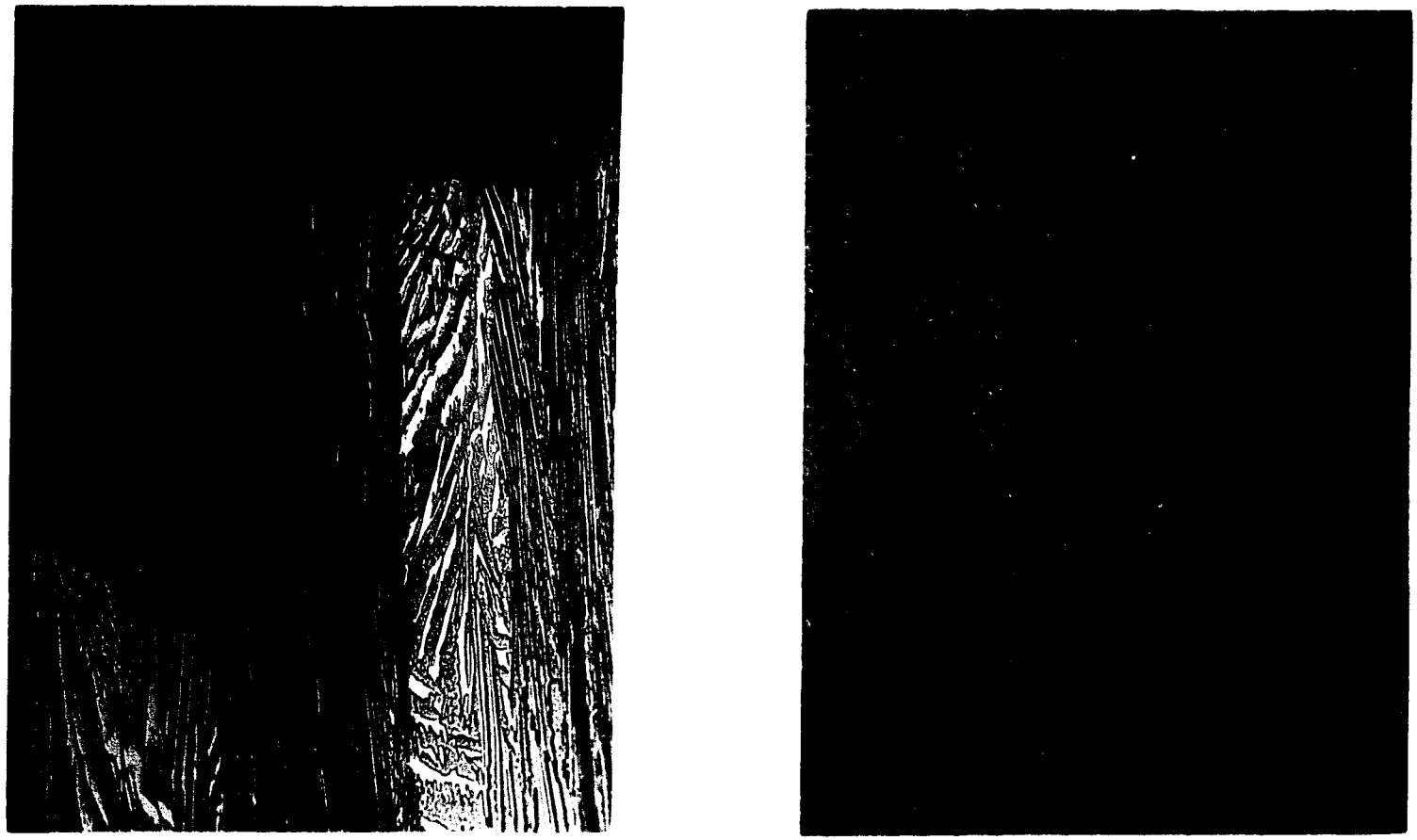

(a) (b)

Figure 13: Longitudinal section of two short time 750°C stress rupture specimens. Electropolished.

(a) Specimen I4-5-1. Note eutectic grain boundary delamination. Magnification 100X.

(b) Specimen J1-5-2. Note the fine distribution of δ twins in δ lamellae. Magnification 1000X.

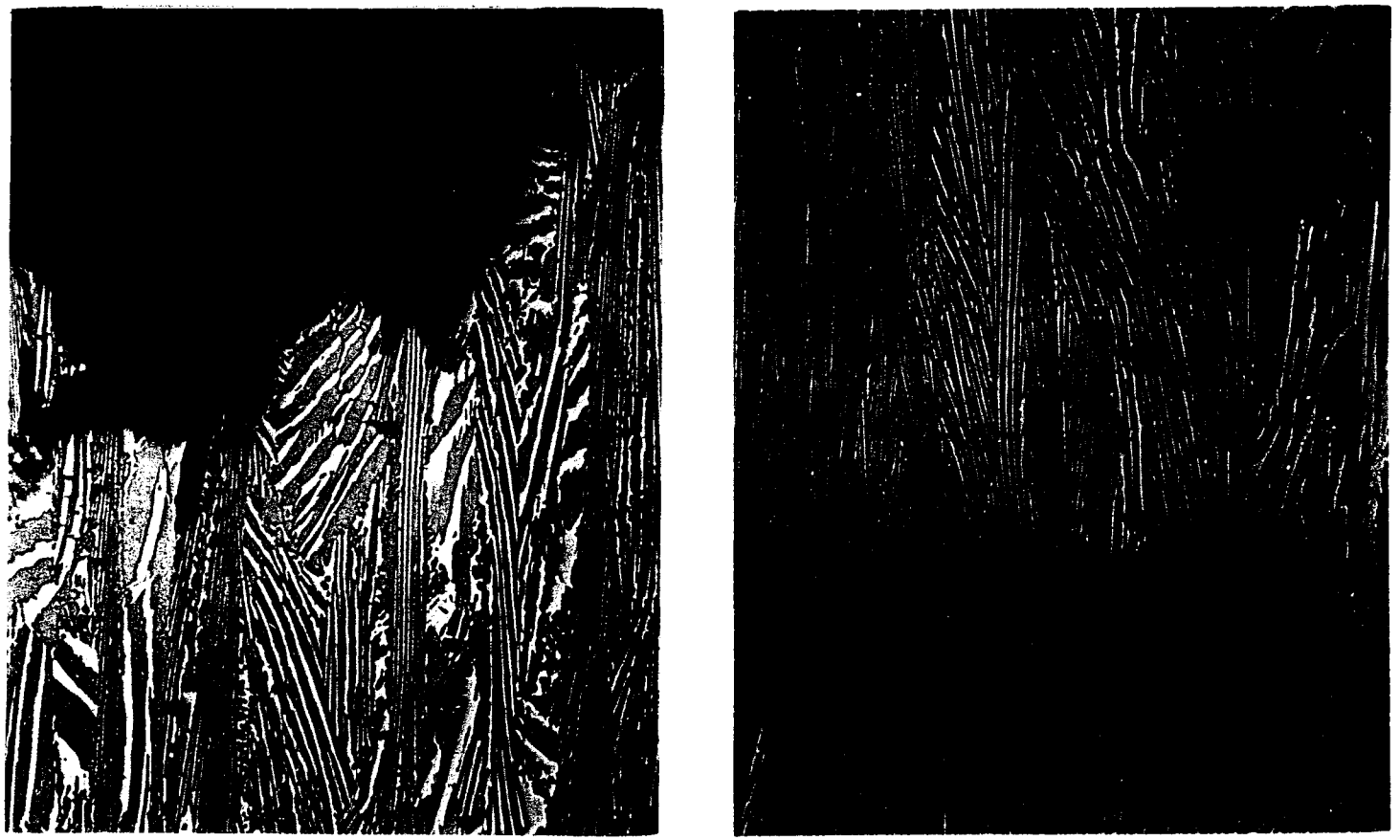

(a) (b)

Figure 14: Longitudinal section of a long time 750°C stress rupture specimen (Specimen J3-5-2) illustrating that fracture was caused by the link-up of voids near the fracture surface. Modified Marbles etchant. Magnification 80X.

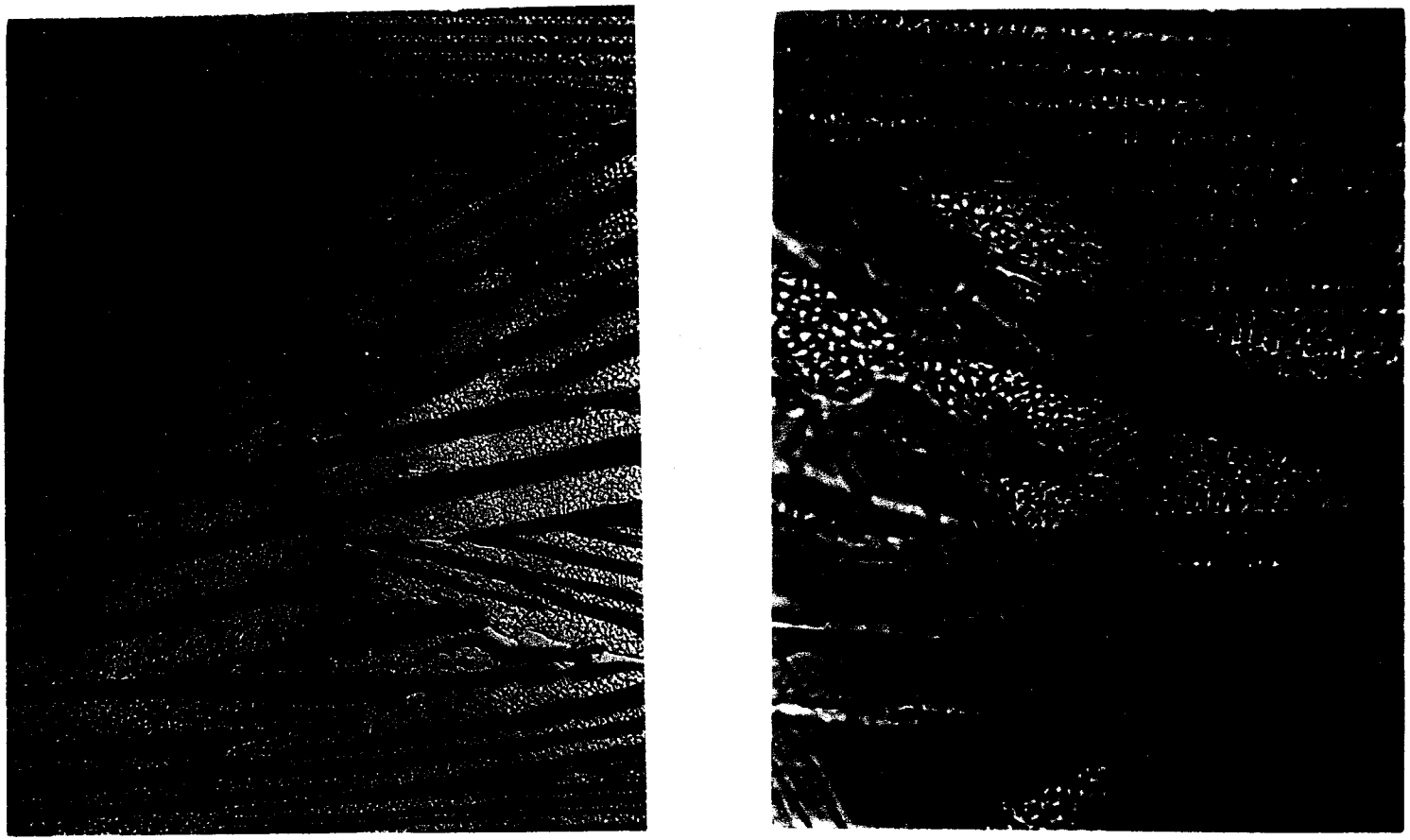

(a) (b)

Figure 15: Longitudinal section of a 760°C stress rupture specimen showing γ-δ cooperative twinning (Specimen I4-5-2). Electropolished.

(a) Note the fine deformation bands away from the fracture surface. Magnification 500X.

(b) Note the cracking occurring near the fracture surface. Magnification 1000X.

Figure 16: Longitudinal photomicrograph of a 760°C stress rupture specimen (Specimen J2-5-1) depicting severe blocky movement of γ and δ lamellae near the fracture surface, producing transgranular cracks. Electropolished. Magnification 1000X.

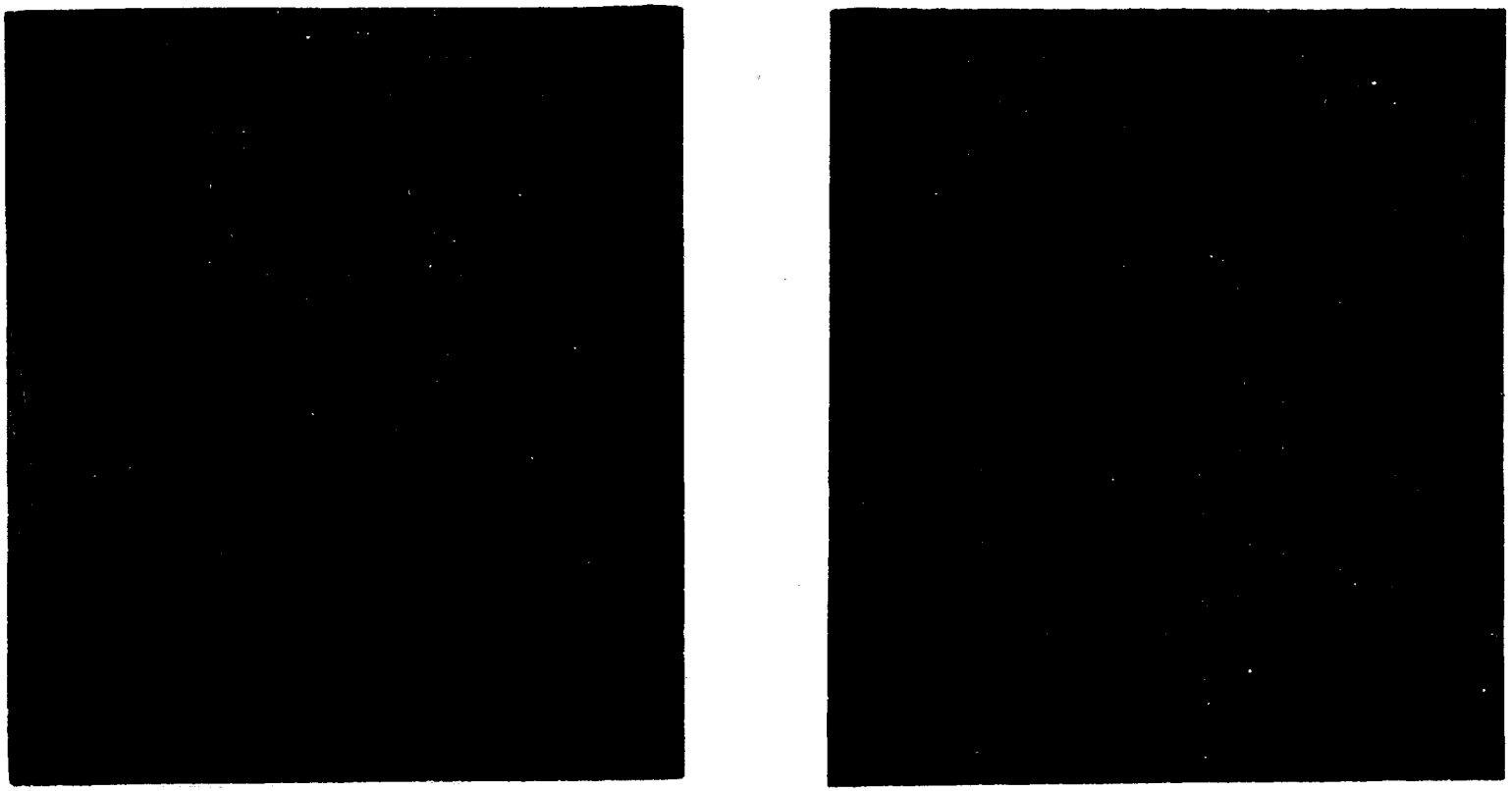

(a) (b)

Figure 17: Longitunal photomicrograph of two 850°C stress rupture specimens.

(a) Specimen J7-5. Note the distribution of voids near the fracture surface (Compare with figure 14b). Modified Marbles etchant. Magnification 80X.

(b) Specimen K4-5. Note the δ phase Widmanstatten precipitates in the γ/γ' lamellae. Electropolished. Magnification 1000X.

(a) (b)

Figure 18: Longitudinal section of a short time 950°C stress rupture specimen (Specimen M5-5-1).

(a) Note cracking in large δ lamellae-Modified Marbles etchant. Magnification 80X.

(b) Electropolished. Magnification 250X.

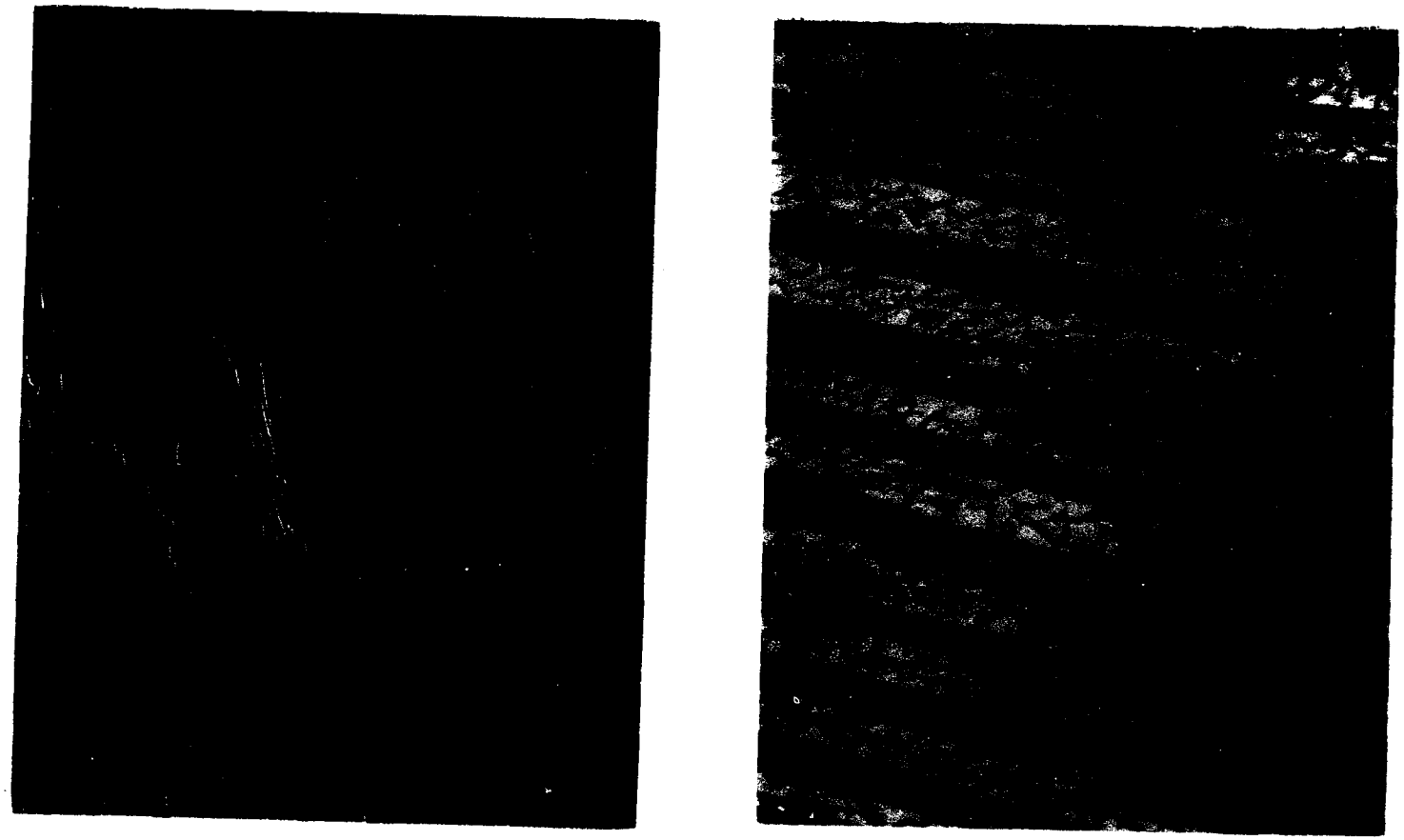

(a) (b)

Figure 19: Longitudinal section of a long time 950°C stress rupture specimen (Specimen I7-5-2).

(a) Note the distribution of large voids near the fracture surface (Compare with figures 14a, 17a and 18a). Modified Marbles etchant. Magnification 80X.

(b) Note the coarsening of the γ' precipitates. Electropolished. Magnification 1000X.

REFERENCES

1. The Superalloys, edited by C. T. Sims and W. C. Hagel, John Wiley & Sons, Inc., New York, 1972.

2. B. J. Piearcey, B. H. Kear, and R. W. Smashey: "Correlation of structure with properties in a directionally solidified nikel-base superalloy", Trans. ASM, 1967, vol. 60, p. 634.

3. B. H. Kear and B. J. Piearcey: "Tensile and Creep Properties of Single Crystals of the Nickel-base Superalloy Mar-M200", Trans. Met. Soc. AIME, 1967, vol. 239, p. 1209.

4. F. L. VerSnyder and M. E. Shank: "The Development of Columnar Grain and Single Crystal High Temperature Materials through Directional Solidification", Mat. Sci. and Engr., 1970, vol. 6, p. 213.

5. F. L. VerSnyder: "Basic Problems Underlying High-Temperature Materials Development", Proc. of Second International Conference on Strength of Metals and Alloys, Asilomar, 1970, p. 1013.

6. R. W. Kraft and D. L. Albright: "Microstructure of Unidirectionally Solidified Al-$CuAl_2$ Eutectic", Trans. Met. Soc. AIME, 1962, vol. 224, p. 1176.

7. R. W. Kraft: "Crystallography of Equilibrium Phase Interfaces in Al-$CuAl_2$ Eutectic Alloys", Trans. Met. Soc. AIME, 1962, vol. 224, p. 65.

8. R. W. Kraft: "The Structure of the Mg-Mg_2Sn Eutectic", Trans. Met. Soc. AIME, 1963, vol. 227, p. 393.

9. F. D. Lemkey, R. W. Hertzberg and J. A. Ford: "The Microstructure, Crystallography and Mechanical Behavior of Unidirectionally Solidified Al-Al_3Ni Eutectic", Trans. Met. Soc. AIME, 1965, vol. 233, p. 334.

10. R. W. Hertzberg, F. D. Lemkey and J. A. Ford: "Mechanical Behavior of Lamellar Al-$CuAl_2$ and Whisker Type Al-Al_3Ni Unidirectionally Solidified Eutectic Alloys", Trans. Met. Soc. AIME, 1965, vol. 233, p. 342.

11. R. W. Kraft, D. L. Albright and J. A. Ford: "Anomalous Thermal Stability of Al-$CuAl_2$ Eutectic Specimens", Trans. Met. Soc. AIME, 1963, Vol 227, p. 540.

12. L. D. Graham and R. W. Kraft: "Coarsening of Eutectic Microstructures at Elevated Temperatures", Trans. Met. Soc. AIME, 1966, vol. 236, p. 94.

13. M. Salkind, G. Leverant and F. George: "Stability of Eutectic Composites Stressed at Elevated Temperatures", J. Inst. Met., 1967, vol. 95, p. 349.

14. Y. Nakagawa and G. C. Weatherly: "The Thermal Stability of the Rod Al_3Ni-Al Eutectic", Acta Met., 1972, vol. 20, p. 345.

15. J. L. Walter and H. E. Cline: "Stability of the Directionally Solidified Eutectics NiAl-Cr and NiAl-Mo", Met. Trans., 1973, vol. 4, p. 33.

16. G. C. Weatherly: "The Stability of Eutectic Microstructures at Elevated Temperatures", Treatise on Materials Science and Technology, vol. 8, Academic Press, New York, 1975.

17. B. J. Bayles, J. A. Ford and M. J. Salkind: "The Effect of Elevated-Temperature Exposure on the Microstructure and Tensile Strength of Al_3Ni Whisker-Reinforced Aluminium", Trans. Met. Soc. AIME, 1967, vol. 239, p. 844.

18. K. D. Sheffer, R. W. Kraft and R. W. Hertzberg: "Microstructure and Crystallography of the Ni-Ni_3Ti Eutectic Alloy", Trans. Met. Soc. AIME, 1969, vol. 245, p. 227.

19. K. D. Sheffler, R. W. Hertzberg and R. W. Kraft: "Elevated-Temperature Mechanical Properties and Fracture Behavior of a Ni-Ni_3Ti Eutectic Alloy", Trans. ASM, 1969, vol. 62, p. 105.

20. R. T. Quinn, R. W. Kraft and R. W. Hertzberg: "Structure and Elevated-Temperature Mechanical Behavior of Unidirectionally Solidified Ni-Ni_3Nb Eutectic Alloy", Trans. ASM, 1969, vol. 62, p. 38.

21. F. D. Lemkey and E. R. Thompson: "Nickel and Cobalt Eutectic Alloys Reinforced by Refractory Metal Carbides", Met. Trans., 1971, vol. 2, p. 1537.

22. P. Annarumma and M. Turpin: "Structure and High Temperature Mechanical Behavior of Ni-Ni_3Nb Unidirectional Eutectic", Met. Trans., 1972, vol. 3, p. 137.

23. R. P. Gangloff: "Elevated Temperature Tensile and Creep Rupture Behavior of the Unidirectionally Solidified Ni-Ni_3Nb Eutectic Cmposite", Master's Thesis, Lehigh University, 1972.

24. R. P. Gangloff and R. W. Hertzberg: "Elevated Temperature Tensile and Creep Rupture Behavior of the Unidirectionally Solidified Ni-Ni_3Nb Eutectic Composite", Proc. of Conference on In Situ Composites, Lakeville, Connecticut, 1972.

25. E. R. Thompson, F. D. George and E. M. Breinan: "The Influence of Interlamellar Spacing on the Strength of the Ni_3Al-Ni_3Cb Eutectic", ibid.

26. W. J. Mills: "Fatigue Crack Propagation Behavior of the Unidirectionally Solidified Ni-Ni_3Nb Eutectic Composite", Master's Thesis, Lehigh University, 1973.

27. F. R. Mollard and M. C. Flemings: "Growth of Composites from the Melt-Part II", Trans. Met. Soc. AIME, 1967, vol. 239, p. 1534.

28. R. M. Jordan and J. D. Hunt: "The Growth of Lamellar Eutectic Structures in Pb-Sn and Al-$CuAl_2$ Systems", Met. Trans., 1971, vol. 2, p. 3401.

29. H. Bibring, J. P. Trottier, M. Rabinovitch, G. Seibel: "Solidification Unidirectionnelle d' Alliages Co-Cr et Ni-Cr Renforcés par des Fibres Monocristallines de TaC. Structure et Propriétés ", Mem. Sci. Rev. Met., 1971, vol. 68, p. 23.

30. E. R. Thompson and F. D. Lemkey: "Unidirectional Solidification of Co-Cr-C Monovariant Eutectic Alloys", Met. Trans., 1970, vol. 1, p. 2799.

31. E. R. Thompson, D. A. Koss and J. C. Chesnutt: "Mechanical Behavior of a Carbide Reinforced Co-Cr Eutectic Alloy", Met. Trans., 1970, vol. 1, p. 2807.

32. E. R. Buchanan and L. A. Tarshis: "Strength and Failure Mechanisms of a Co-15 Cr-13 TaC Directionally Solidified Eutectic Alloy", Met. Trans., 1974, vol. 5, p. 1413.

33. H. Bibring, G. Seibel and M. Rabinovitch: "Renforcement des Composites à Fibres, Obtenus en Solidification Orientée, par Durcissement Structural de la Matrice", C. R. Acad. Sc., 1971, vol. 271, p. 1521.

34. H. Bibring, E. Seibel and M. Rabinovitch: "Nouveaux Développements dans l' Etude des Superalliages à Fibres Obtenus par Solidification Dirigée", Mem. Sc. Rev. Met., 1972, vol. 69, p. 341.

35. J. L. Walter and H. E. Cline: "Structures and Properties of Cobalt Base-TaC Eutectic Alloys", Met. Trans., 1973, vol. 4, p. 1775.

36. E. R. Buchanan and L. A. Tarshis: "Carbide Reinforcement in Two Directionally Solidified Alloyed Nickel Eutectic Alloys", Met. Trans., 1973, vol. 4, p. 1895.

37. F. D. Lemkey: "Eutectic Superalloys Strengthened by δ, Ni_3Cb Lamellae and γ', Ni_3Al Precipitates", NASA CR-2278, UARL, Nov. 1973.

38. F. D. Lemkey and E. R. Thompson: "Eutectic Superalloys Strengthened by δ, Ni_3Cb Lamellae, γ', Ni_3Al Precipitates and Reduced Interlamellar Spacing", Proc. of the Third International Conference on the Strength of Metals and Alloys, Cambridge, England, vol. 1, 1973.

39. M. Gell and R. H. Barkalow: "Microstructure-Property Relationships of a Directionally Solidified Superalloy Eutectic", ibid.

40. H. R. Bertorello, R. W. Hertzberg and R. W. Kraft: "Hot Tensile Properties and Deformation Response of a γ(Ni)/ γ'(Ni_3Al)- δ(Ni_3Nb)", to be published in Proceedings of Second Conference on In Situ Composites, Bolton Landing, Spetember, 1975.

41. E. M. Breinan: "Eutectic Composites", Final Technical Report Contract N000 14-71-C-0393, United Technologies Research Center, December, 1975.

42. G. R. Leverant and B. H. Kear: "The Mechanism of Creep in Gamma Prime Precipitation-Hardened Nickel-Base Alloys at Intermediate Temperatures", Met. Trans., 1970, vol. 1, p. 491.

43. R. Kossowsky: "Creep Behavior of Ni-Cr Lamellar Eutectic Alloy", Met. Trans., 1970, vol. 1, p. 1909.

44. E. M. Breinan, E. R. Thompson and W. K. Tice: "Creep Behavior of Al-Al_3Ni Eutectic Composites", Met. Trans., 1970, vol. 1, p. 211.

45. E. M. Breinan, E. R. Thompson, G. P. McCarthy and W. J. Herman: "Microstructural Characteristics of the Directionally-Solidified Al-Al_3Ni Eutectic and Their Influence on Creep Fracture", Met. Trans., vol. 1, p. 221.

46. F. Garofalo: "Fundamentals of Creep and Creep Rupture in Metals", The McMillan Company, New York, 1965.

47. N. S. Stoloff and R. G. Davies: "Mechanical Properties of Ordered Alloys", Prog. Mat. Sci., vol. 13, p. 3.

48. Reference 32 cited in reference 42.

49. H. R. Bertorello, R. W. Hertzberg, W. Mills, R. W. Kraft and M. Notis: "Solubility Limits and Precipitation Phenomena in Ni-Ni_3Nb Aligned Eutectic", Acta Met., 1976, vol. 24, p. 271.

VITA

Xuan Nguyen-Dinh was born the son of Mr. and Mrs. Bang Nguyen-Dinh on February 23, 1949, in Saigon, Viet Nam. He received his elementary and secondary education from Lycée Jean-Jacques Rousseau (Saigon) and was graduated in May, 1967.

In January, 1972, Mr. Nguyen-Dinh was graduated from Ecole Polytechnique Fédérale (Lausanne, Switzerland) with a degree "Diplôme d'Ingénieur Mécanicien". During the year 1972, he was employed as an assistant in the "Institut de Machines Hydrauliques", then worked at the "Institut des Métaux et Machines" during the year 1973. He began graduate study at Lehigh University in January, 1974, under a scholarship awarded by Brown Boveri Research Center (Baden, Switzerland).

In June, 1976, Mr. Nguyen-Dinh was married to the former Stephanie A. Thompson in the Washington Temple of the Church of Jesus Christ of Latter-day Saints.